Radiocarbon dating of planktonic foraminifer shells: A cautionary tale

Figen Mekik [1]

Received 26 June 2013; revised 26 November 2013; accepted 1 December 2013; published 15 January 2014.

[1] Sedimentation rate, bioturbation, winnowing, and calcite dissolution produce significant radiocarbon age offsets among multiple species of coexisting planktonic foraminifers and pteropod fragments. We compare the radiocarbon age of foraminifer species and pteropod fragments with estimates of percent calcite dissolved made with a sedimentary proxy (*Globorotalia menardii* fragmentation index—MFI) to delineate the effect of dissolution on radiocarbon age of foraminifers. Data from two core top transects on the Rio Grande Rise (RIO) and Ontong Java Plateau (OJP) and from down core sediments of varying sedimentation rates in the tropical Pacific (ME-27, MD98 2177, and MW91-9 56GGC) reveal that sediments with the greatest accumulation rates produce the least age offsets among coexisting species. Age offsets among coexisting foraminifers are about 3500 years on RIO, and 1000 years on OJP. Two core tops from RIO yield an age of the Last Glacial Maximum possibly due to mass displacement of younger sediments downslope. Foraminifer age increases with increasing dissolution and there is a consistent pattern of older foraminifer fragments coexisting with younger whole shells of the same species. The only exception is sediments which have experienced high dissolution where fragments are younger than whole shells. The age offset between fragments of *G. menardii* and its coexisting whole shells does not exceed the age offset among other coexisting foraminifer species in the same core tops.

Citation: Mekik, F. (2014), Radiocarbon dating of planktonic foraminifer shells: A cautionary tale, *Paleoceanography*, *29*, 13–29, doi:10.1002/2013PA002532.

1. Introduction

[2] Paleoceanographers working on sediments going back as far as 30,000 years rely on radiocarbon dates to develop age models for their cores [e.g., *Stuiver et al*., 1998]. Radiocarbon dating has other applications, such as using age differences between coexisting planktonic and benthic foraminifers to infer changes in the strength of deep ocean circulation [e.g., *Broecker and Clark*, 2010], ventilation [*Broecker et al*., 2004; *Keigwin*, 2004], stratification [*Sikes et al*., 2000], and ages for water masses [*Waelbroeck et al*., 2001]. Recently, *Barker et al*. [2007] and *Broecker and Clark* [2011] showed significant differences in ages of various coexisting planktonic foraminifers in core top sediments. This phenomenon complicates interpretations of the geologic record and confounds understanding the full extent and magnitude of geological events preserved in sediments. We present new radiocarbon age results from both core tops and down core work in order to explore the magnitude and causes behind age offsets among coexisting planktonic foraminifers.

1.1. Background

1.1.1. Mechanisms of Mixing

[3] Figure 1 provides a summary of the various mechanisms that result in "mixed signals" among the radiocarbon ages of different components within sediments. *Barker et al*. [2007] considered two broad categories for mechanisms of mixing and age offset among coexisting foraminifers: processes within the sedimentary bioturbated zone and processes associated with the dissolution, secondary calcification, and differential dissolution of foraminifer tests within the sediments. Other mechanisms to explain the variations in age among coexisting foraminifers include variations in faunal assemblages through time, downslope transport, variations in atmospheric ^{14}C activity, habitat depth differences among planktonic foraminifer species, and sediment focusing.

1.1.2. Previous Work

[4] The action of benthic organisms living in the upper few centimeters of sediments causes the sediments to be mixed; this process is termed *bioturbation*. This mixing action obscures paleoceanographic signals that may be retrieved from various sedimentary components [*Peng et al*., 1977; *Peng and Broecker*, 1984; *Bard et al*., 1987; *Barker et al*., 2007].

[5] In their seminal work, *Peng and Broecker* [1984] showed that the age difference between coexisting benthic and planktonic organisms may be confounded as a result of bioturbation, and that the signal to be measured from the foraminifer tests could be shifted back in time. They calculated that the amount by which the sedimentary signal is obscured by bioturbation

[1]Department of Geology, Grand Valley State University, Allendale, Michigan, USA.

Corresponding author: F. Mekik, Department of Geology, Grand Valley State University, Allendale, MI 49401, USA. (mekikf@gvsu.edu)

0883-8305/14/10.1002/2013PA002532

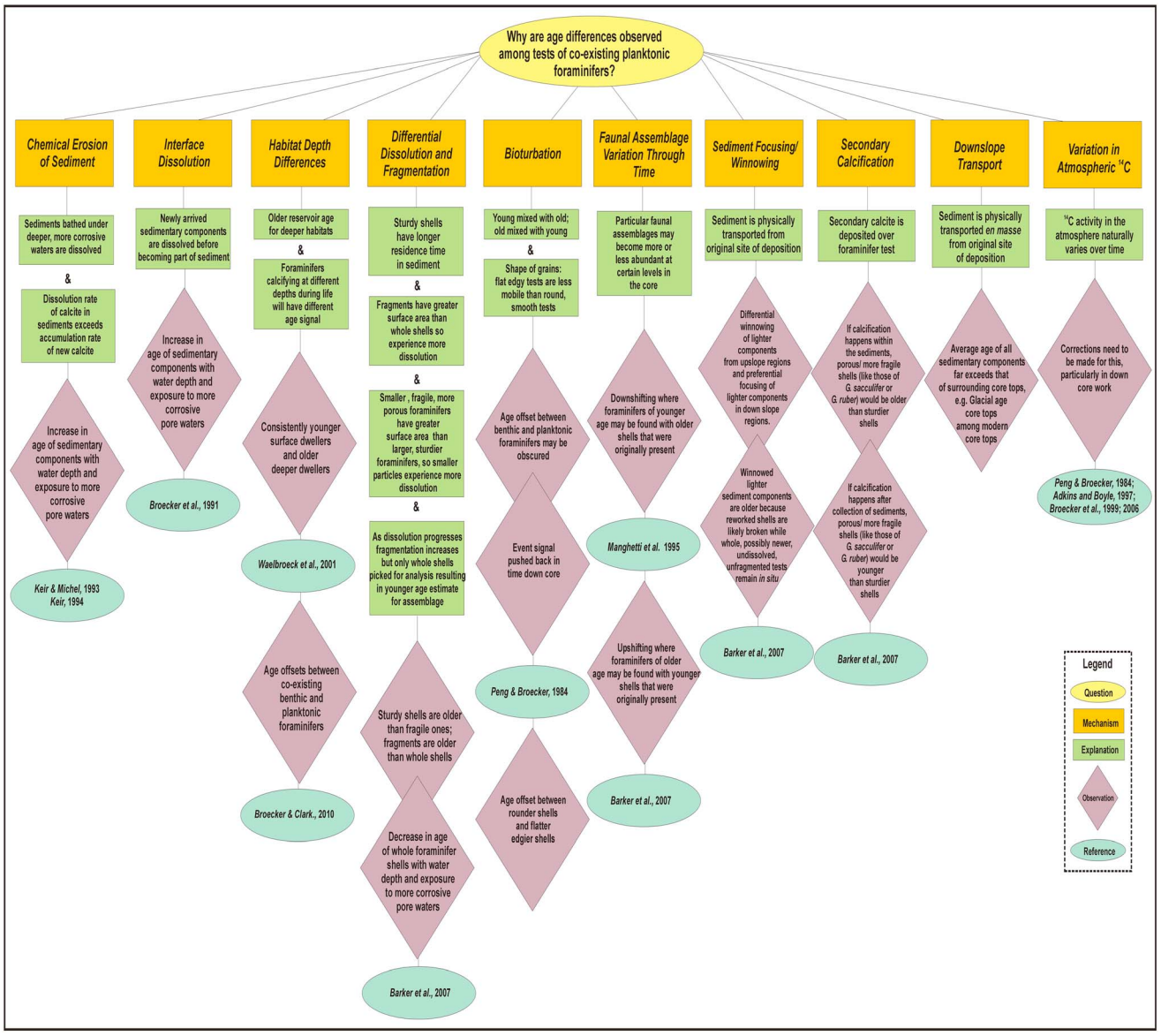

Figure 1. Summary of mechanisms that may cause age offset among multiple coexisting components of deep sea sediments.

is inversely proportional to the rate of sedimentation. In other words, in cores with high resolution due to high sediment accumulation rates, the age differences between planktonic and benthic foraminifers are less compromised by bioturbation.

[6] Bioturbation can also obscure boundaries of event horizons in the sedimentary record by reworking the sedimentary components carrying the signal for a given event. Changes in faunal abundances within the sedimentary record form a good example [*Barker et al*., 2007]. If a particular taxon becomes more abundant at a certain time (horizon), the fossils of this taxon may be reworked into lower sediments (down-working) thereby giving a younger average age estimate to older sediments when these younger, down-worked fossil shells are picked for dating [*Manighetti et al*., 1995]. Similarly, the sedimentary horizon where the abundance of a particular taxon is reduced may be obscured by reworking sedimentary components upward in the sequence (up-working), wherein older ages may be attributed to younger sediments above the horizon if the up-worked older fauna are dated [*Barker et al*., 2007].

[7] *Keir and Michel* [1993] and *Keir* [1984] illustrated through modeling and radiocarbon data that *chemical erosion* can play a significant part in causing the core top age of sediments to increase as dissolution in sediments increases with water depth. Where the rate of calcite dissolution exceeds the rate of calcite accumulation, chemical erosion of the younger sediment may occur. As a result, older sedimentary particles will be brought into the bioturbated layer which would increase the average radiocarbon age of the core tops.

[8] Another related mechanism is *interface dissolution* [*Broecker et al*., 1991] which posits that newly arriving calcite particles are preferentially dissolved before becoming part of the sedimentary record thereby increasing the residence time of particles already incorporated into the sediment. This process too would increase the radiocarbon age of highly dissolved core top samples.

[9] *Berger* [1970] published a ranking for 22 planktonic foraminifer species based on the resistance of shells to dissolution within sediments. While this seems like a subtle issue, as *Barker et al*. [2007] point out, it can become important if shells of foraminifers dissolve at different rates, and bioturbation mixes fragments and whole shells of differentially preserved tests. If *differential dissolution* of foraminifer shells is a dominant mechanism, radiocarbon ages would be generally biased toward younger components of the sediment because the shells that are newly arriving into the sediment would not have yet dissolved, while older components would have dissolved somewhat and eventually fragmented [*Barker et al*., 2007]. Because whole shells are generally preferred for radiocarbon analyses, the newly arrived, thick, heavy, and unfragmented shells would be more likely picked for analysis which would then bias age estimates toward younger values.

[10] *Broecker and Clark* [2011] showed that among shells of species that have experienced high levels of dissolution, age differences among coexisting specimens can be commonly as high as 1000 years. Conversely, if the preferential fragmentation of porous and fragile foraminifer shells (like those of *Globigerinoides ruber* or *Globigerinoides sacculifer*) due to dissolution within the sediments leads to shorter residence times for whole shells of these species in the bioturbated zone, then the foraminifers picked for radiocarbon analysis will be those with sturdier shells which are likely older than coexisting shells from more fragile foraminifers [*Broecker and Clark*, 2011].

1.1.3. Model Predictions and Results

[11] The one-dimensional model created by *Barker et al*. [2007] calculates potential effects of fragmentation and differential dissolution of foraminifer tests within the sedimentary mixed layer. This low-order model assumes homogeneous dissolution where percent calcite dissolved is defined as the percentage of raining calcium carbonate that is dissolved. Chemical erosion of sediments previously deposited on the seabed or interface dissolution are not included in model calculations.

[12] The model by *Barker et al*. [2007] makes numerous predictions: (1) dissolution of shells and fragmentation should drive the radiocarbon age estimates made from whole shells toward younger ages by significant amounts (more than 1000 years) particularly in cores with sedimentation rates less than 3 cm/kyr; (2) the largest radiocarbon age offset between bulk sediment and whole shells should occur when dissolution reaches about 50%; (3) fragments of foraminifers should be 3–4000 years older than their whole shell counterparts; (4) fragments of species with sturdier shells should be older than those with more fragile/porous shells; and (5) individual species ages in core tops should decrease with increasing dissolution related to increasing water depth.

[13] *Barker et al*. [2007] found an age offset of 2200 years among coexisting species of planktonic foraminifers within sediments accumulating at a rate of 3 cm/kyr. In their results from a core in the South China Sea, tests from a robust species (*Pulleniatina obliquiloculata*) consistently gave older ages than a more fragile shelled species (*G. sacculifer*) by about 900 years, as predicted by their model [*Barker et al*., 2007]. However, their results from core tops on the Ontong Java Plateau were more complicated. The radiocarbon data from five species of planktonic foraminifers (both their whole shells and fragments) showed that fragments of robust shelled foraminifer species were about 2300 years older than their whole shelled counterparts as predicted by the model; but contrary to model predictions, the ages of whole shells of individual species increased with dissolution, while whole shells from fragile species were consistently older than those from robust species [*Barker et al*., 2007].

1.2. Research Questions

[14] The discussion above paints an alarming picture for the reliability of radiocarbon dating and paleoceanographic applications based on these ages. Previous studies restricted core top work on the effect of calcite dissolution on radiocarbon age of foraminifers to the Pacific Ocean [e.g., *Barker et al*., 2007; *Broecker and Clark*, 2011]. We present results of radiocarbon age offset among several species of coexisting planktonic foraminifers (their whole shells and fragments) from both core tops in the Atlantic Ocean (Rio Grande Rise) and the Pacific Ocean (Ontong Java Plateau) along depth transects where dissolution increases downslope. We compare radiocarbon ages of multiple coexisting planktonic foraminifers and pteropod fragments to estimates of percent calcite dissolved by using the *Globorotalia menardii* fragmentation index (MFI) [*Mekik et al*., 2002, 2010] as a quantitative indicator of calcite dissolution within sediments. Lastly, we present data from down core work where radiocarbon ages among multiple planktonic foraminifer species and their fragments are compared in three cores from the Pacific Ocean each with different sediment accumulation rates.

[15] Our research questions are as follows:

[16] 1. Do radiocarbon ages of shells of single planktonic foraminifer species increase with increasing dissolution as modeled by *Keir and Michel* [1993], do they show clear age offsets as posited by the interface dissolution hypothesis of *Broecker et al*. [1991], or do they decrease with increasing dissolution through homogeneous dissolution as modeled by *Barker et al*. [2007]?

[17] 2. Do changes in sediment accumulation rate and bioturbation, both among core tops and in down core work, affect the age offset between whole shells of different planktonic foraminifer species? If so, how much?

[18] 3. Does the age difference between fragments and whole shells of the same species change in a consistent way with increasing calcite dissolution; or is this masked by differential dissolution of shells and sediment focusing in even fast accumulating cores? This question is particularly important for *G. menardii* shells because MFI is based on counting fragments and whole shells of this species.

[19] 4. How is the reliability and usefulness of MFI affected by age differences between whole shells of *G. menardii* and its fragments?

1.3. *Globorotalia menardii* Fragmentation Index

[20] The *G. menardii* fragmentation index (MFI) is a proxy and transfer function developed by *Mekik et al*. [2002, 2010] to estimate the percent calcite dissolved within a deep sea sediment sample. MFI is based on the ratio of the number of whole *G. menardii* specimens (W) to the number of damaged specimens (D) of this species within a sediment sample, such that $MFI = D/(D + W)$. The MFI transfer function is the quantitative relationship between model-derived estimates of percent calcite dissolved and the fragmentation trend of *G.*

Table 1. Core Information for All Samples Used in This Study[a]

Region	Core	Latitude	Longitude	Water Depth (m)	MFI	Bottom Water $\Delta CO_3^=$ (μmol/kg)
			Core Tops			
OJP	ERDC 90	−0.865	157.48	1903	0.42	11.5
OJP	ERDC 121	−0.183	158.713	2245	0.33	5.17
OJP	ERDC 127	−0.003	161.418	3724	0.83	−13.24
RIO	AII 107-9 69	−31.658	−36.023	2158	0.08	42.81
RIO	AII 107-9 66	−31.945	−36.205	2716	0.22	37.59
RIO	AII107-9 132	−30.838	−38.283	3343	0.16	25.32
RIO	CHN 115-6 92	−30.428	−38.838	3934	0.24	−4.88
RIO	AII 107-9 142	−30.947	−39	4148	0.6	−14.67
RIO	AII 107-9 133	−30.85	−38.402	3454	0.28	18.41
RIO	AII 107-9 149	−30.89	−38.563	3744	0.21	−1.37
			Down Core			
Region/Core	Core Depth (cm)	Latitude	Longitude	Water Depth (m)	MFI	Ave. Sed. Rate (cm/kyr)
OJP/ MW91-9-56	2.5	0	158	4041	0.898	1.01
	26.5				0.73	1.82
	38.5				0.61	1.73
WEP/ MD98-2177	6	1.403	119.078	968	0.25	12
	345				0.27	55.67
	475					50.1
EEP/ ME-27	0.5	−1.853	−82.787	2203	0.71	0.91
	10.5				0.68	26.3
	80.5				0.31	7.12
	125.5				0.15	7.09

[a]OJP = Ontong Java Plateau; RIO = Rio Grande Rise; WEP: Western Equatorial Pacific; EEP = Eastern Equatorial Pacific.

menardii shells in core tops of marine sediments from tropical and subtropical regions of three ocean basins (Pacific, Atlantic, and Indian) [*Mekik et al*., 2010]. The model used to calibrate MFI is Muds and was developed by *Archer et al*. [2002]. The MFI calibration relationship is shown in equation (1) [*Mekik et al*., 2002, 2010, $R^2 = 0.80$]. See *Mekik et al*. [2002, 2010] for detailed information about the calibration sample set, modeling, development, transfer function, and error margins of MFI.

$$\%\,CaCO_3\text{Dissolved} = -4.0081 + (\text{MFI} \times 113.87) - (\text{MFI}^2 \times 37.879) \quad (1)$$

[21] MFI is a bulk sediment dissolution proxy because all three factors that drive calcite dissolution in deep sea sediments are incorporated into its calibration equation (equation (1)). These three factors are bottom water carbonate ion undersaturation, organic carbon flux to the deep sea and calcite flux to the seabed. In regions of high surface ocean productivity, the ratio of organic carbon to calcite flux (also known as the *rain ratio*) plays an important role in driving calcite dissolution in sediments [*Emerson and Bender*, 1981; *Archer and Maier-Reimer*, 1994]. The core tops used herein are part of MFI's calibration sample set, and MFI data from these core tops (Table 1) was previously published by *Mekik et al*. [2002, 2010].

[22] Bottom water carbonate ion undersaturation is presented as $\Delta CO_3^=$ (delta calcite), which is defined by Equation (2). Where $\Delta CO_3^=$ is positive, the sediment is above the water depth where $[CO_3^=]$ is at saturation with respect to calcite solubility (saturation horizon), and calcite is less likely to dissolve; where $\Delta CO_3^=$ is negative, sediment is below the saturation horizon, and calcite is more likely to dissolve.

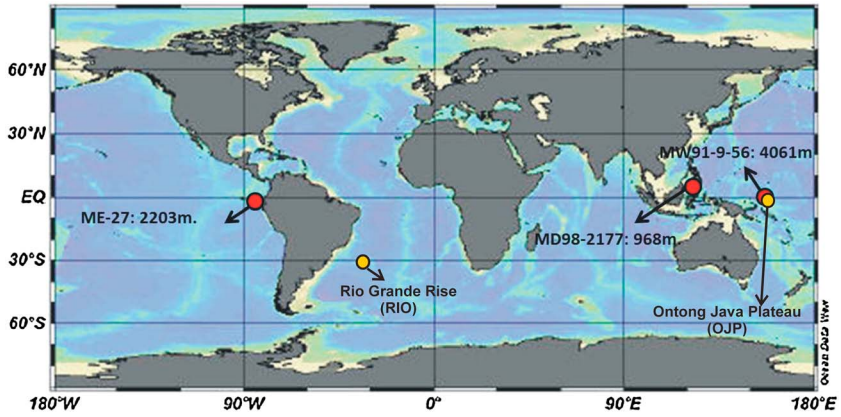

Figure 2. Core and transect locations depicted over map of world ocean bathymetry (map was generated with Ocean Data View software).

Table 2. Information for Fossilized Organisms Used in This Study[a]

Organism	Habitat Designation in Text	Species	Shell Type	Habitat Depth (m)	References for Habitat Depth	Whole Shells Dated?	Frags Dated?	$\Delta^{14}C$ in Core Top or Downcore Sample?
Planktonic foraminifer	Surface Dweller	*Globigerinoides sacculifer*	porous/ fragile	0–80	*Bijma* [1991] *Spero and Lea* [1993] *Anand et al.* [2003]	yes	no	core top/ down core
Planktonic foraminifer	Surface Dweller	*Globigerinoides ruber*	porous/ fragile	0–50	*Anand et al.* [2003] *Sadekov et al.* [2009]	yes	no	core top
Planktonic foraminifer	Deep Dweller Thermocline	*Globorotalia menardii*	sturdy	75	*Be* [1960] *Farmer et al.* [2007]	yes	yes	core top/ down core
Planktonic foraminifer	Deep Dweller Thermocline	*Globorotalia truncatulinoides*	sturdy	200–500	*Anand et al.* [2003]	yes	no	core top
Planktonic foraminifer	Deep Dweller Thermocline	*Pulleniatina obliquiloculata*	sturdy	50–125	*Anand et al.* [2003] *Sadekov et al.* [2009] *Farmer et al.* [2007]	yes	yes	core top/ down core
Planktonic foraminifer	Deep Dweller Thermocline	*Neogloboquadrina dutertrei*	sturdy	50–100 (DCM)	*Anand et al.* [2003] *Fairbanks et al.* [1982] *Fairbanks and Wiebe* [1980] *Loubere* [2001]	yes	no	core top/ down core
Pteropod	Deep Dweller	variable	-	50–650	*Jasper and Deuser* [1993] *Juranek et al.* [2003]	no	yes	core top/ down core

[a]DCM = Deep Chlorophyll Maximum.

$$\Delta CO_3^{=} = [CO_3^{=}]_{in\ situ} - [CO_3^{=}]_{at\ saturation} \quad (2)$$

[23] Strong data reproducibility for MFI was demonstrated in repeated counts by several individuals and published in the work of *Mekik et al*. [2010]. The error margin associated with repeated counts is ± 0.04 MFI units which yields ± 1% error in estimating % calcite dissolved [*Mekik et al*., 2010]. MFI estimates $\Delta CO_3^{=}$ of bottom waters with a predictive error of ± 10 μmol/kg, and MFI estimates percent calcite dissolved with an average predictive error of ± 7% calcite dissolved [*Mekik et al*., 2010].

[24] The MFI has been compared to other calcite dissolution proxies, such as size normalized foraminifer shell weight (SNSW) and Mg/Ca of foraminifer tests, in both core top [*Mekik and François*, 2006; *Mekik et al*., 2007a, 2010; *Mekik and Raterink*, 2008] and down core work [*Mekik et al*., 2012]. Most recently, *Doss and Marchitto* [2013] generated down core MFI data and compared MFI with the B/Ca proxy which is used as an indicator of past seawater carbonate ion saturation.

[25] *Mekik and Raterink* [2008] provided an extensive discussion on the comparison of SNSW to MFI, where both proxies trace dissolution relatively well, but where the ability of SNSW to trace dissolution is compromised by the effects of $[CO_3^{=}]$ of foraminifer habitat waters on their shell thickness. This point was also raised and demonstrated by *Barker and Elderfield* [2002]. *Mekik and Raterink* [2008] found no effect of habitat $[CO_3^{=}]$ on MFI. Figure 10 in the work of *Mekik et al*. [2010] is a direct comparison of the ability of SNSW and MFI to trace bottom water $[CO_3^{=}]$ where both proxies do this well. *Mekik and François* [2006] and *Mekik et al*. [2007a] both showed that MFI and the Mg/Ca in shells of multiple species of planktonic foraminifers have a strong relationship in core tops where overlying sea surface temperatures are constant and calcite dissolution is the only parameter affecting foraminifer Mg/Ca.

2. Methods

2.1. Sampling

[26] We address our research questions by using core top samples from two depth transects, one on the Rio Grande Rise (RIO) in the southwest Atlantic Ocean (seven-sediment samples) and one on the Ontong Java Plateau (OJP) in the western equatorial Pacific (three-sediment samples). All core top samples are from gravity cores and sediment aliquots of 1 g from the top 0–2 cm of the core. The depth transects for the core tops used herein were chosen specifically in locations far removed from areas of high surface ocean productivity so as to minimize the effect of the rain ratio on dissolution and to isolate bottom water carbonate ion undersaturation as the primary driver of calcite dissolution at our sampling locations. This approach minimizes errors introduced by uncertainties in rain ratios for our sampling locations created by the paucity of data for organic carbon and calcite rain in the world ocean.

[27] *Mekik et al*. [2010] calculated $\Delta CO_3^{=}$ using Global Data Analysis Project (GLODAP) bottle data [*Key et al*., 2004; *Sabine et al*., 2005] and Ocean Data View Software [*Schlitzer*, 2008]. The relationship between MFI and bottom water $\Delta CO_3^{=}$ among its 89 core top calibration samples is

Table 3. Core Top $\Delta^{14}C$, Raw Radiocarbon Age, and $\delta^{13}C$ Data

Core	*G. sacculifer* Whole Shells	*G. ruber* Whole Shells	*G. menardii* Whole Shells	*G. trunc* Whole Shells	*P. obliqui.* Whole Shells	Pteropod Fragments	*G. menardii* Fragments	*P. obliqui.* Fragments
				$\Delta^{14}C$ (‰)				
ERDC 90	−410.3 ± 1.81		−378.7 ± 1.4		−426.7 ± 1.12			
ERDC 121	−365.4 ± 1.5		−198.1 ± 0.64		−395 ± 1.76		−449.5 ± 1.96	−444.7 ± 1.68
ERDC 127			−381 ± 3.08		−440.9 ± 1.73		−390.3 ± 2.11	−412.2 ± 1.89
AII 107-9 69		−348.5 ± 2.19	−371.7 ± 2.07			−468.6 ± 1.85		
AII 107-9 66		−443.9 ± 2.31	−452.1 ± 1.98	−407.9 ± 1.93		−509.9 ± 3.43	−475.7 ± 2.81	
AII107-9 132		−568.4 ± 3.42	−451.1 ± 1.56	−386.2 ± 1.38			−536.5 ± 3.13	
CHN 115–6 92		−551.9 ± 2.71	−510 ± 1.77	−422.8 ± 1.47			−621.5 ± 3.78	
AII 107–9 142			−598.4 ± 3.28	−618.6 ± 4.87			−518.9 ± 3.24	
AII 107–9 133		−875.9 ± 7.76	−892 ± 8.26	−874.8 ± 6.29			−932.4 ± 13.79	
AII 107–9 149		−900 ± 12.6	−908.3 ± 7.92	−905.4 ± 7.66			−933.8 ± 9.87	
				Raw Radiocarbon Age				
ERDC 90	4,240 ± 35		3,820 ± 30		4470 ± 20			
ERDC 121	3,650 ± 35		1,770 ± 25		4040 ± 35		4,800 ± 35	4720 ± 30
ERDC 127					4670 ± 30		3,970 ± 45	4270 ± 35
AII 107-9 69		3,440 ± 50	3,730 ± 45			5080 ± 30		
AII 107-9 66		4,710 ± 40	4,830 ± 35	4,210 ± 35		5730 ± 55	5,190 ± 45	
AII107-9 132		6,750 ± 50	4,820 ± 25	3,920 ± 30			6,180 ± 45	
CHN 115-6 92		6,450 ± 40	5,730 ± 30	4,410 ± 25			7,800 ± 50	
AII 107-9 142			7,330 ± 45	7,740 ± 60			5,880 ± 50	
AII 107-9 133		16,750 ± 70	17,900 ± 75	16,700 ± 60			21,600 ± 120	
AII 107-9 149		18,500 ± 110	19,200 ± 70	18,950 ± 70			21,800 ± 85	
				$\delta^{13}C$ (‰)				
ERDC 90	1.94		1.75		1.15			
ERDC 121	1.88		1.62		1.18		1.3	1.03
ERDC 127					1.17		1.94	1.38
AII 107-9 69		0.75	1.35			2.2		
AII 107-9 66		1.29	1.61	1.47		1.74	0.81	
AII107-9 132		1.08	1.64	1.39			0.51	
CHN 115-6 92		1.06	1.49	1.55			1.59	
AII 107-9 142			1.41	0.71			1.26	
AII 107-9 133		0.94	1.18	1.02			1.13	
AII 107-9 149		0.85	1.36	1.01			1.39	

Table 4. Down Core $\Delta^{14}C$, Raw Radiocarbon Age, and $\delta^{13}C$ Data

Core	Core Depth (cm)	*G. sacculifer* Whole Shells	*N. dutertrei* Whole Shells	Pteropod Fragments	*G. menardii* Whole Shells	*P. obliqui.* Whole Shells	*G. menardii* Fragments	*P. obiqui* Fragments
				$\Delta^{14}C$ (‰)				
MW91-9 56	2.5				−340.4 ± 1.55	−475.4 ± 2.08	−505.1 ± 1.55	−446.6 ± 2.82
MW91-9 56	26.5	−803.8 ± 10.65			−845.4 ± 5.47	−819.7 ± 5	−866.8 ± 7.16	−840.5 ± 10.01
MW91-9 56	38.5				−926.7 ± 7.59	−926.2 ± 8.79	−932.6 ± 12.45	−935 ± 17.26
MD98-2177	6	−66.2 ± 0.38			−86.5 ± 0.35			
MD98-2177	345	−648.1 ±3.68		−668.3 ± 5.04	−628.5 ± 3.05	−656.9 ±4.02	−657.8 ± 6.92	
MD98-2177	475	−737.3 ± 6.17		−760.7 ± 3.81	−739.6 ± 4.26	−738 ± 6.76	−733.8 ± 6.62	
ME-27	0.5		−249 ± 1.06				−319.6 ± 3.24	
ME-27	10.5				−321.2 ± 1.85		−376 ± 3.19	
ME-27	80.5		−781.4 ± 5.36		−783.7 ± 9.78		−795.9 ± 7.02	
ME-27	125.5		−885.2 ± 7.71		−882.2 ± 11.23			
				Raw Radiocarbon Age				
MW91-9 56	2.5				3340 ± 35	5180 ± 35	5650 ± 35	4750 ± 50
MW91-9 56	26.5	13,100 ± 100			15,000 ± 55	13,750 ± 45	16,200 ± 65	14,750 ± 95
MW91-9 56	38.5				21,000 ± 70	20,900 ± 70	21,700 ± 100	22,000 ± 150
MD98-2177	6	550 ± 45			725 ± 30			
MD98-2177	345	8,390 ± 45		8,860 ± 60	7,950 ± 40	8590 ± 50	8,610 ± 85	
MD98-2177	475	10,750 ± 70		11,500 ± 40	10,800 ± 45	10,750 ± 70	10,650 ± 75	
ME-27	0.5		2300 ± 35					
ME-27	10.5						3,790 ± 70	
ME-27	80.5		12,200 ± 55		12,300 ± 100		12,750 ± 70	
ME-27	125.5		17,400 ± 70		17,200 ± 100			
				$\delta^{13}C$ (‰)				
MW91-9 56	2.5				1.86	1.23	1	1
MW91-9 56	26.5	1.5			1.78	1.15	1.99	−0.18
MW91-9 56	38.5				1.99	1.43	2.1	1.28
MD98-2177	6	1.8			1.45			
MD98-2177	345	1.61		0.4	1.11	0.35	0.5	
MD98-2177	475	1.51		0.16	1.24	0.05	0.72	
ME-27	0.5		1.32					
ME-27	10.5						1.03	
ME-27	80.5		1.05		0.87		0.5	
ME-27	125.5		1.42		1.63			

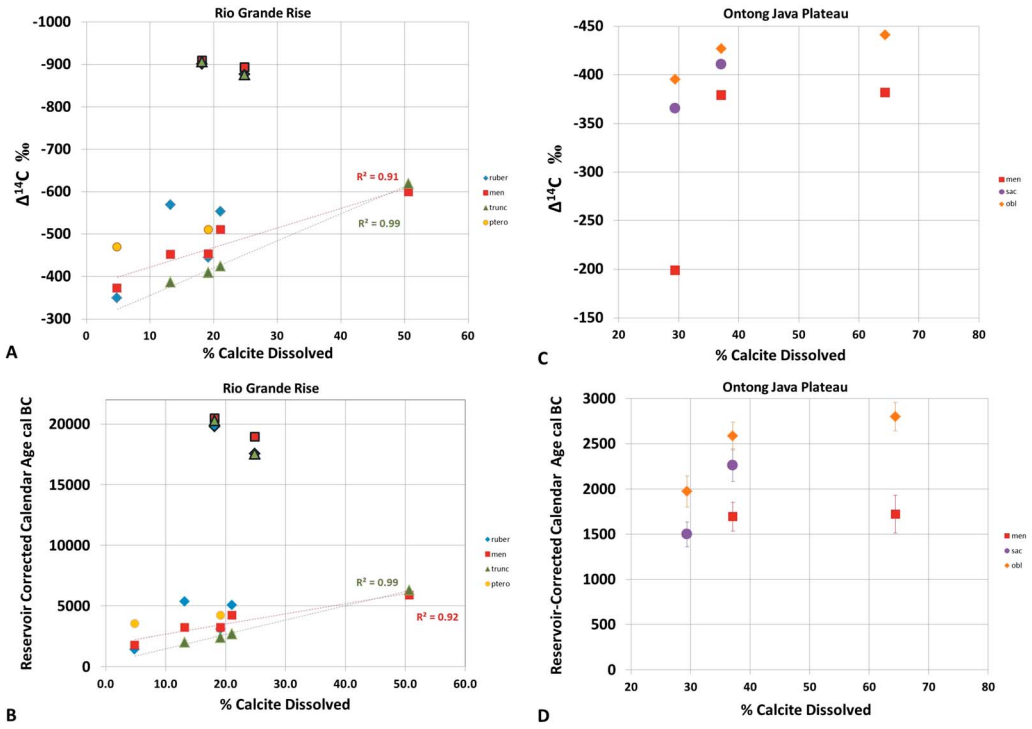

Figure 3. The $\Delta^{14}C$ and calendar age (cal BC) data plotted against MFI-based percent calcite dissolved for whole foraminifer species in core tops from the Rio Grande Rise and Ontong Java Plateau. Data points of LGM age are highlighted with a dark rim. Statistical calculations shown are based on the trend of the five non-LGM samples. ruber = *Globigerinoides ruber*; men = *Globorotalia menardii*; trunc = *Globorotalia truncatulinoides*; ptero = Pteropod fragments; sacc = *Globigerinoides sacculifer*; and obl = *Pulleniatina obliquiloculata*.

strong with an R^2 of 0.82 in Atlantic core tops and 0.9 in Pacific core tops [see *Mekik et al*., 2010, Figure 5]. The relationship between MFI and $\Delta CO_3^=$ in the subset used herein ($R^2 = 0.72$) is similar to the calibration relationship of MFI and $\Delta CO_3^=$.

[28] We present down core radiocarbon age data from three cores in the equatorial Pacific (two cores in the west and one in the east; MD98 2177, MW91-9-56GGC, and ME 24, respectively—Figure 2 and Table 1). We studied various species of planktonic foraminifers with different resistance to dissolution and pteropod fragments which are made of aragonite (Table 2). The aragonite saturation horizon is significantly shallower than the calcite saturation horizon in the water column in all tropical and subtropical ocean basins (GLODAP database) [*Key et al*., 2004].

2.2. Radiocarbon Dating

[29] Radiocarbon and $\delta^{13}C$ data from pteropod fragments, whole planktonic foraminifer tests from multiple species, and species-specific foraminifer fragments were generated at the National Ocean Sciences Accelerator Mass Spectrometry Facility (NOSAMS) of Woods Hole Oceanographic Institution. All radiocarbon ages shown in figures herein have been corrected for reservoir offsets and calendar years through the CALIB 6.0 software [*Stuiver and Reimer*, 1993; http://calib.qub.ac.uk/calib/]. Reservoir ages were calculated using the MARINE database linked to CALIB 6.0 (http://calib.qub.ac.uk/marine/). This marine calibration database includes a global ocean reservoir correction of 400 years and accommodates for local effects through a ΔR parameter. ΔR is defined as the difference in reservoir ages of local regions and the model global ocean. Constant values of reservoir corrections were used for core tops on RIO, on OJP, and each of our down core locations. Tables 3 and 4 list raw radiocarbon age data and associated error margins, as reported by NOSAMS. Radiocarbon data shown in Figures 3–6 are presented as both $\Delta^{14}C$ and as reservoir corrected calendar ages (cal BC). The $\Delta^{14}C$ was calculated using the fraction modern defined by equation (3).

$$\text{Fraction Modern} = \frac{^{14}C\,/\,^{12}C \text{ of sample (‰)}}{^{14}C/^{12}C \text{ of modern (‰)}} \quad (3)$$

[30] The $\Delta^{14}C$ was calculated using the fraction modern as in equation (4) [*Stuiver and Polach*, 1977].

$$\Delta^{14}C\,(‰) = \left(\text{Fraction Modern} * e^{\lambda(1950 - Y_c)} - 1\right) * 1000 \quad (4)$$

Where $\lambda = 1/$ true mean life of radiocarbon = 0.00012097; and Y_c = year of collection of sample.

[31] For fossil samples, Y_c is assumed to be 0, so equation (4) becomes equation (5) [*Stuiver and Polach*, 1977]. We used equation (5) to calculate $\Delta^{14}C$ for our samples.

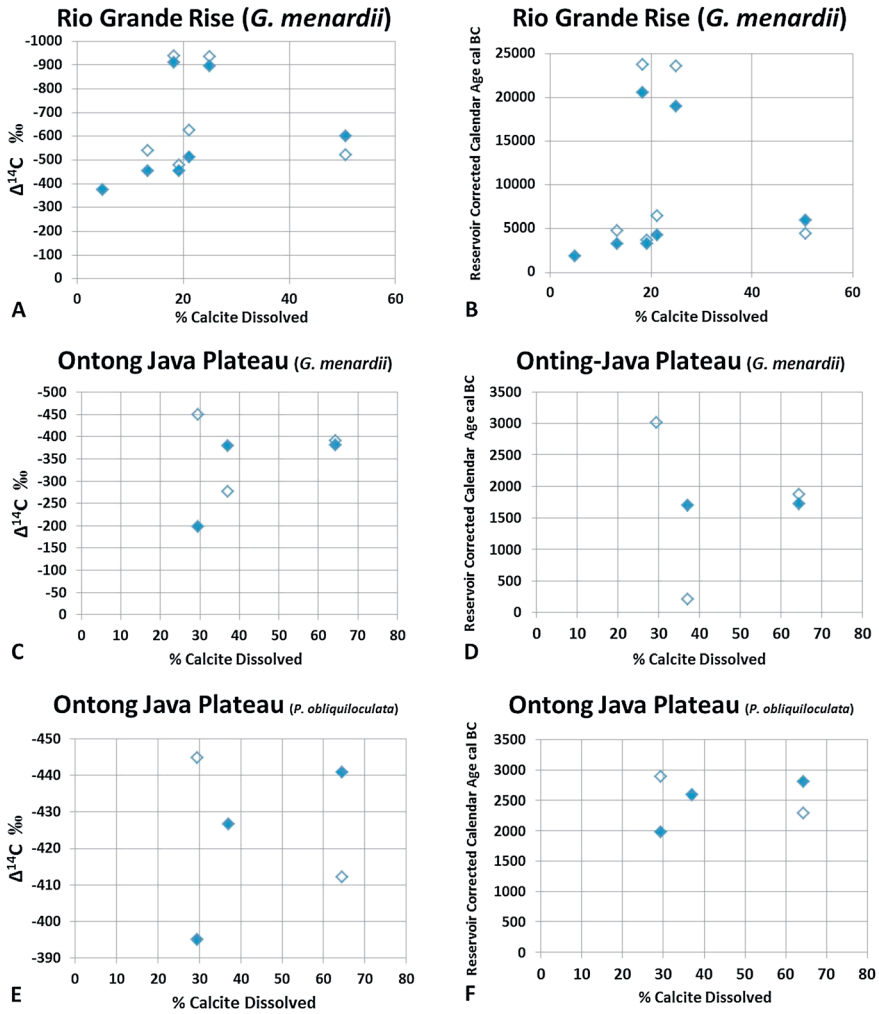

Figure 4. The $\Delta^{14}C$ and calendar age (cal BC) data plotted against MFI-based percent calcite dissolved for species of whole foraminifers and fragments of foraminifers in core tops from the Rio Grande Rise and Ontong Java Plateau. Open diamonds represent fragments of the species designated in the title of each panel. Filled diamonds represent whole shells of the same species.

$$\Delta^{14}C\,(‰) = (\text{Fraction Modern} - 1)*1000 \qquad (5)$$

[32] In reporting $^{14}C/^{12}C$ data, NOSAMS corrects for the assumption that the fractionation of ^{14}C relative to ^{12}C is double that of ^{13}C by measuring $\delta^{13}C$ from all samples. Then calculations of fraction modern are corrected to the value it would have if its original $\delta^{13}C$ were $-25‰$ which is the $\delta^{13}C$ value to which all radiocarbon measurements are normalized at NOSAMS. The $\delta^{13}C$ data for our samples, as reported to us by NOSAMS, are listed in Tables 3 and 4. The error associated with $\delta^{13}C$ correction from a stable mass spectrometer is approximately 0.1‰ (for further details of calculations, see http://www.whoi.edu/nosams/page.do?pid=40146).

[33] NOSAMS employs the accelerator mass spectroscopy method of radiocarbon analysis and utilizes the VG Prism Stable Mass Spectrometer for making $\delta^{13}C$ measurements. See the NOSAMS web site for detailed information about instrumentation, measuring protocols, error estimation, and calculation of fraction modern (http://www.whoi.edu/nosams/page.do?pid=40146).

2.3. Sediment Accumulation Rates and Mixed Layer Depths for RIO and OJP

[34] *Berger and Killingley* [1982] estimated 0.8–2.4 cm/kyr for the sediment accumulation rate on OJP and 5–8 cm for the mixed layer depth there. The age of the mixed layer with radiocarbon analyses on box cores from OJP (in close proximity to our core tops) range from 3400 to 4800 years [Table IV, page 99 in *Berger and Killingley*, 1982]. Sediment accumulation rates are also low on RIO with a previously published value of 1.85 cm/kyr [*Jones et al.*, 1984] (specifically for sample AII 107–9 69GGC also used herein see Table 1). The sediment mixing depths in the Vema Channel alongside RIO is estimated to be greater than 8 cm [*Berger et al.*, 1977; *Peng et al.*, 1977]. This yields an average age for the mixed layer of 4300 years on RIO.

3. Results

3.1. Core Top Results

[35] Two of the seven core top samples on RIO show radiocarbon ages corresponding to the Last Glacial Maximum in

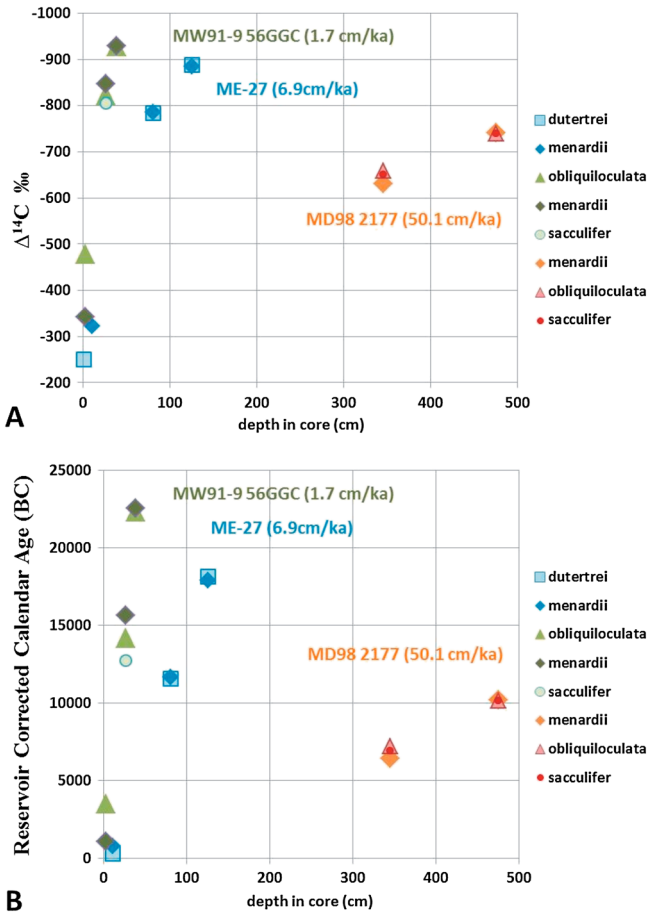

Figure 5. The $\Delta^{14}C$ and calendar age (cal BC) data plotted against sediment depth in core for multiple species of whole planktonic foraminifers in ME-27 (*Neogloboquadrina dutertrei* and *Globorotalia menardii*), MW91-9 56 GGC (*G. menardii, Pulleniatina obliquiloculata*, and *Globigerinoides sacculifer*), and MD98 2177 (G. *menardii, P. obliquiloculata*, and *G. sacculifer*).

three foraminifer species (Figures 3a and 3b and Table 3), *G. ruber*, *G. menardii*, and *Globorotalia truncatulinoides*. As a result, we exclude these two anomalously old core tops from analysis of the relationship between radiocarbon age of foraminifers and increasing MFI-based calcite dissolution along the depth transect on RIO.

[36] As a general trend among the remaining five core tops on RIO, foraminifer age increases with increasing % calcite dissolved as measured with MFI. Specifically, radiocarbon ages of *G. menardii* and *G. truncatulinoides* shells have strong linear trends with increasing percent calcite dissolved on RIO (Figures 3a and 3b). Pteropods are generally the oldest components of the sediments on this transect. In three core tops on RIO, *G. ruber*, a porous and fragile species, is the youngest foraminifer; but *G. ruber* is the oldest foraminifer in two other samples. *G. sacculifer*, another species with porous and fragile shells, is older than *G. menardii* in two of the three samples on OJP; and *P. obliquiloculata* is consistently older than *G. menardii* on this transect.

[37] The increase in species-specific foraminifer age with increasing calcite dissolution is also discernable in those from OJP (Figures 3c and 3d). The combined range of MFI in core tops is 0.08–0.83 (Table 1) in both transects and corresponds to a range of 5–65% calcite dissolved (equation (1)) and −14.67 to 42.81 μmol/kg of $\Delta CO_3^=$ (Table 1). Specifically, in Figure 3a we see a strong linear relationship between the $\Delta^{14}C$ of *G. menardii* and *G. truncatulinoides* with % calcite dissolved, R^2 is 0.91 and 0.99, respectively.

[38] Radiocarbon age for fragments and whole shells of *G. menardii* on RIO, and *G. menardii*, and *P. obliquiloculata* on OJP (Figure 4) show that ages of fragments are generally older than those of coexisting whole shells of the same species. The exception is in samples that have experienced high dissolution such as the *G. menardii* fragments in the sample on RIO with the highest % dissolved (Figures 4a and 4b) and *P. obliquiloculata* fragments in the sample on OJP with the highest % dissolved there (Figures 4e and 4f).

3.2. Down Core Results

[39] All foraminifer species, at each sampling horizon, produce very similar ages to one another in all three cores except MW 91–9 56GGC which has the lowest sedimentation rate (Figure 5). Down core records of radiocarbon age for whole shells and fragments (Figure 6) reveal that fragments are consistently either the same age or older than whole shells. Age offsets are most extreme in the low sedimentation rate core, MW91-9 56GGC.

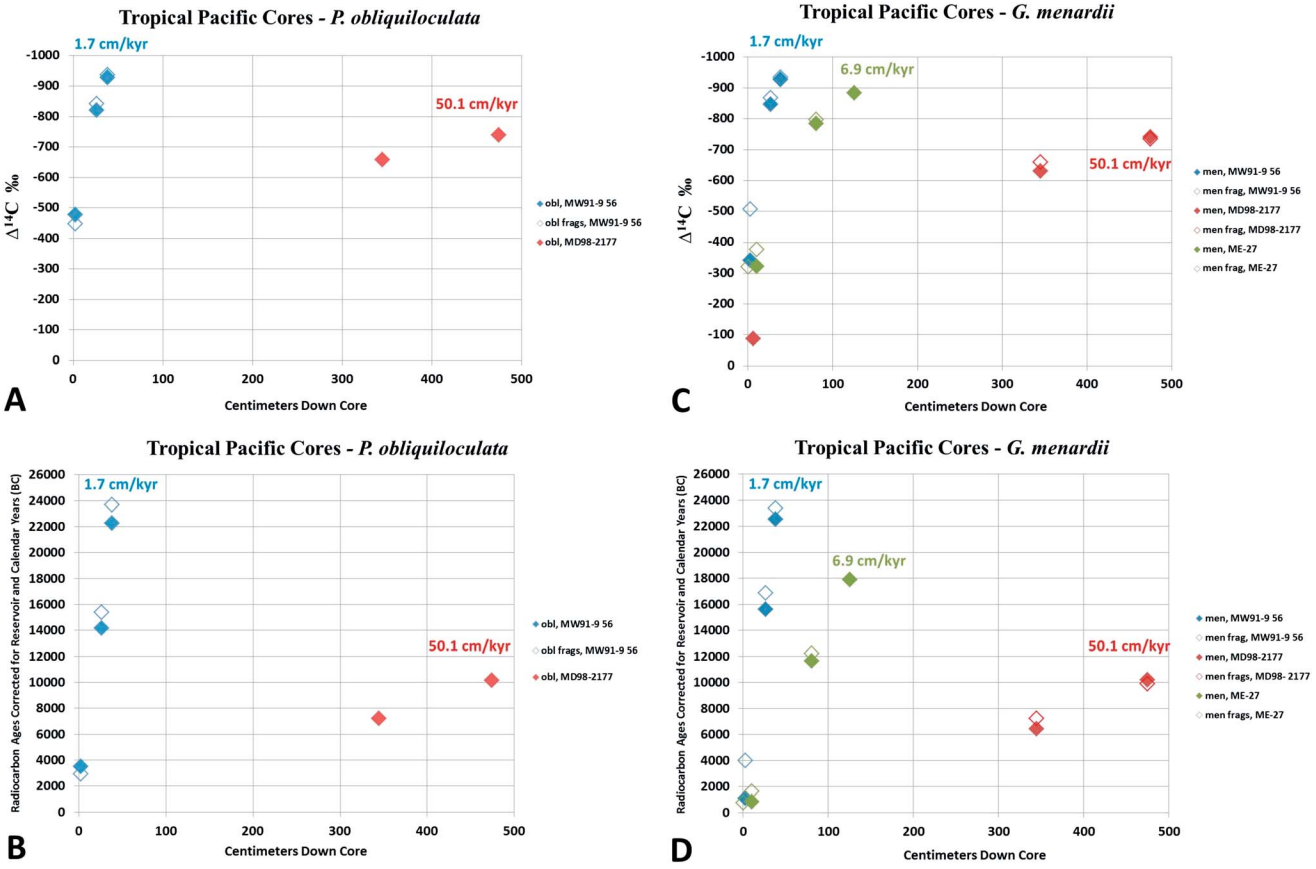

Figure 6. The $\Delta^{14}C$ and calendar age (cal BC) data plotted against sediment depth in core for species of whole foraminifers and fragments of foraminifers in cores ME 27, MW91-9 56GGC and MD98 2177. Open diamonds represent fragments; closed diamonds represent whole shells. men = *Globorotalia menardii*; men frag = fragments of *G. menardii*; obl = *Pulleniatina obliquiloculata*; and obl frags = fragments of *P. obliquiloculata*.

4. Discussion

4.1. Relationship Between $\Delta^{14}C$ and Calcite Dissolution in Sediments

[40] The increase of radiocarbon age of bulk sediment with water depth is a well-known conundrum in equatorial Pacific sediments [*Keir*, 1984; *Broecker et al*., 1991; *Oxburgh*, 1998; *Barker et al*., 2007]. The trend of increasing age of individual foraminifer species with dissolution supports the chemical erosion mechanism of *Keir and Michel* [1993] and *Keir* [1984] although it says nothing about the age differences among coexisting planktonic foraminifers. Our data do not support the model expectations from *Barker et al*. [2007] that foraminifer age would decrease as dissolution increases. However, *Barker et al*. [2007] also observed in their core tops from OJP that foraminifers become older as dissolution increases.

[41] Average age for the mixed layer can be calculated with equation (6) from *Keir and Michel* [1993].

$$\text{Average Age of Mixed Layer} = \frac{\text{Mixed Layer Thickness}}{\text{Sediment Accumulation Rate}} \quad (6)$$

[42] The cores on RIO have low sediment accumulation rates compared to other subtropical open ocean areas (1.85 cm/kyr from *Jones et al*. [1984]). If we assume a mixed layer depth of 8 cm as is suggested for RIO [*Berger et al*., 1977; *Peng et al*., 1977], then based on equation (6), a net sediment accumulation rate decrease from 2 cm/kyr in shallow sites to 1 cm/kyr in deeper sites due to increased calcite dissolution would double the average age of mixed layer sediments. Thus, the best explanation for the increase in radiocarbon age of planktonic foraminifers with increasing calcite dissolution is the chemical erosion mechanism.

4.2. Age Differences Between Sturdy and Fragile Foraminifer Shells

[43] *Barker et al*. [2007] observed that foraminifer species with porous, more fragile tests are older than sturdier shells of other coexisting planktonic foraminifer species by up to 2200 years although their model predicted that porous fragile shells of these species should be the youngest. Our results are mixed.

[44] On OJP (Figures 3c and 3d), tests of *G. sacculifer* are older than those of *G. menardii* but younger than those of *P. obliquiloculata*. On RIO (Figures 3a and 3b), *G. ruber* is the oldest among foraminifers in two samples out of seven core tops. It is the youngest species in three samples one of which is the core top in shallowest water and two of which are of LGM age (Table 3). These mixed results suggest that possibly

more than one mechanism is at play, such as a combination of differential dissolution, winnowing, and bioturbation.

[45] The observation that *G. ruber* is the youngest foraminifer in three of seven core tops from RIO can be explained by *Barker et al.'s* [2007] modeling results. *G. ruber* shells are more porous than shells of most other foraminifer species and therefore have more surface area for dissolution. The longer *G. ruber*s stay in the sediment, the more likely they will be to dissolve compared to their sturdier counterparts. In three samples where *G. ruber*s are the youngest, we suppose that whole shells of this species were likely those newly becoming incorporated into the sediment and did not have enough time to dissolve. Therefore they are younger than other coexisting foraminifer species.

[46] It is difficult to explain the observation that fragile porous shells, like those of *G. ruber* and *G. sacculifer*, are sometimes the oldest component of the sediment. *Barker et al*. [2007] suggested that because foraminifer shells come with varying shell thickness and calcification [*Barker and Elderfield*, 2002], individuals of all species may have different susceptibility to dissolution even within the same species. Additionally seasonal changes in the concentration of the carbonate ion in habitat waters may cause different populations of the same species with varying shell thickness to coexist in the death assemblage within sediments [*Barker et al*., 2007]. Dissolution will remove the fragile, lighter shells more rapidly, and sturdier shells will have longer residence time in the sediments giving older ages when picked for analysis. This could be one viable explanation for why porous/fragile shells are the oldest foraminifer species in a sample; but it does not explain how foraminifers with fragile shells (like *G. ruber*) can be the oldest in sediments that experienced little dissolution where younger shells should be more abundant (like in our RIO core tops AII 107–9 132 and CHN 115–6 92).

[47] An explanation for porous, fragile shells being the oldest in core tops that experienced little calcite dissolution may be that the preferential winnowing of newly arriving lighter, porous shells remove the younger individuals from sediment before they permanently become part of the sedimentary record. Simultaneously, bioturbation may work up older individuals of the same species from deeper sedimentary layers to the core top. This hypothesis remains to be tested with sedimentary indicators, but is the best explanation for our observations on RIO.

[48] The lack of *G. ruber* or *G. sacculifer* tests as well as pteropod fragments in the deepest samples from both RIO and OJP which have experienced the most dissolution (MFI = 0.6 and 0.83, respectively; see Table 1) suggests that fragile foraminifer shells and aragonitic pteropod fragments are probably being completely dissolved. The absence of these fragile foraminifer species at greater depths has also been documented by *Barker et al*. [2007], and *Broecker and Clark* [2010, 2011].

4.3. Sediment Accumulation Rate and Bioturbation

[49] Shallower core tops that experienced little calcite dissolution show the greatest offset in ages of coexisting planktonic foraminifers and pteropod fragments (~2000–3500 years in Figure 3). This is a clear indication of intensive bioturbation and mixing in these sediments.

[50] If there is a gradient to faunal assemblages down core, then vertical mixing can create large age offsets among coexisting components of the sediment. *Barker et al*. [2007, Figure 6] presented down core foraminifer assemblage counts for a core on the OJP (MW91-9 BC36) in close proximity to those used herein where they observed no down core faunal gradient. Similar data are not available from the RIO at this time but future studies on RIO may reveal large changes in faunal assemblages down core that could explain the large age offset among coexisting species of foraminifers we observe from core tops there.

[51] Why are rounder and smoother shells, such as those of *P. obliquiloculata*, generally older than those of coexisting *G. menardii* which are flat and edgy although both live at thermocline depths in the water column (Table 2)? This is particularly evident in OJP core tops (Figures 3c and 3d). We posit that the preferential mobility of *P. obliquiloculata* shells during bioturbation would be greater than those of *G. menardii* shells due to the round shape and smooth shell of the former and the flat and edgy shape of the latter. *G. menardii* shells would not be as easily worked up or down through the sediment column as those of *P. obliquiloculata* and may therefore reflect the most accurate age for the sediment sample. Also *G. menardii* are less vulnerable to dissolution than most other species [*Berger*, 1970].

[52] We performed a simple, iterative calculation to simulate the effects of bioturbation on different components of the sediment, and to test whether this hypothesis is realistic (P. Loubere, personal communication, 2013). Bioturbation is a function of sedimentation rate, mixing rate, and mixed layer depth (equation (6)). Sedimentation rate or mixed layer depth (the depth to which benthos move about and stir sediment) would not be different for various components of the sediment at the same location. The mixing rate is the only variable that may be different from one type of sediment component to another.

[53] To simplify the calculation, we assumed two extreme cases. One for a species which does not mix at all and progressively accumulates on the seabed (species A), and another that mixes rapidly through the bioturbation zone (species B). The age difference between the two species would come from mixing up of older sediment within the bioturbation zone, and the residue of even older sediments from previously existing bioturbation zones. The lower the sedimentation rate, the greater this mixing effect will become.

[54] In our calculations, we assumed a mixed layer depth of 8 cm and a sedimentation rate of 2 cm/kyr in keeping with the published values for these parameters on OJP [*Berger and Killingley*, 1982]. We created a hypothetical sediment profile divided into 8 sections of 1 cm depth each. We used midpoint ages for each 1 cm—thick layer as an initial condition (depicted by the blue curve labeled "no bioturbation" in Figure 7a). We also assumed that we move forward in time by 500 years for each iteration of our simulation of bioturbation. The following four steps were performed in each iteration: (1) add a 1-cm top layer of midpoint age of 250 years; (2) shift the previous layers downward and age them by 500 years; (3) mix the layers in pairs by taking the average of the midpoint ages in each pair of layers from bottom of the stack of layers upward (ensuring the same number of layers as the initial condition); and (4) repeat steps 1 through 3 until the age profile stabilizes which is defined by the average age of the mixed layer becoming a constant value.

[55] The stabilization of the age profile required 24 iterations in this calculation (Figure 7a). The no bioturbation

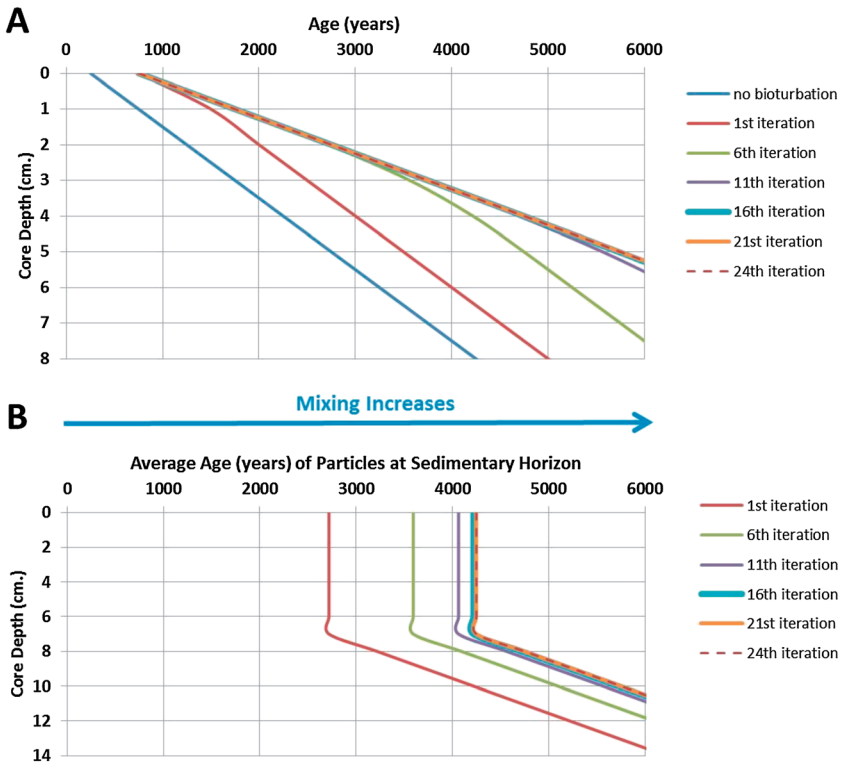

Figure 7. (a) Evolution of age profiles with progressive mixing of the sediments. The no bioturbation curve reflects the starting conditions for the subsequent iterations. (b) Profile of average mixed layer age and average age of sedimentary components within each subsequent horizon based on the age profile calculations presented in Part A. Homogeneous average mixing age is assumed for the age of horizons within the mixed layer. See text for details of calculations.

curve in Figure 7a represents the age profile for species A which does not mix at all. Species B, which we theorized to be extremely mobile, would hypothetically have the age profile of the 24th iteration. In Figure 7b we plotted the average mixed layer age throughout the mixed layer in each iteration. It shows the stabilization of the average mixed layer age at 4200 years after 24 iterations. This mixed layer age is in keeping with that for OJP (3400–4800 years) published by *Berger and Killingley* [1982].

[56] According to our crude simulation of bioturbation and assumed values of mixing depth and sedimentation rate, the age difference between species A and a thoroughly mixed species, such as species B, is about 500–1500 years in the top 2 cm of the sediment column from where our core tops were sampled. This is consistent with the age offsets we see among our foraminifers on OJP and suggest that our hypothesis is realistic. Differential mobility of foraminifer species may be at least a partial cause of age-offsets among coexisting foraminifers. More data allowing for more sophisticated calculations are needed to test this hypothesis.

[57] Our down core results reflect the effect of bioturbation also. In cores with high sediment accumulation rates (ME-27 and MD28-2177 in Figure 5), whole shells of various coexisting species of foraminifers have similar $\Delta^{14}C$ with one another. Whereas, in core MW91-9 56GCC sedimentation rate is low, and the age offset among coexisting foraminifers is large (~2000–3000 years and −320 to −490‰ in $\Delta^{14}C$). Care must be taken to find cores with high sedimentation rate (>3 cm/kyr based on the *Barker et al.* [2007] modeling results) and low dissolution in order to yield the most accurate age estimates as also suggested by others [e.g., *Broecker and Clark*, 2010, 2011; *Barker et al.*, 2007].

4.4. The $\Delta^{14}C$ Differences Between Fragments and Whole Shells: Differential Dissolution, Sediment Focusing, or Both?

[58] *Le and Thunnell* [1996] showed that foraminifer species with sturdy, robust tests dominate foraminifer assemblages as dissolution increases. Increased dissolution of foraminifer shells causes thinning of shells and whole shell weight loss before fragmentation begins [*Broecker and Clark*, 2001]. Taking these two observations together and the modeling results of *Barker et al.* [2007], it is reasonable to predict that foraminifer fragments should be older than their coexisting whole shell counterparts. We observe this phenomenon consistently across both our core top (Figure 4) and down core samples (Figure 6).

[59] However, two samples do not follow this prediction: one on RIO that has experienced the most dissolution (AII 107–9 142GGC, MFI = 0.6, *G. menardii* fragments are younger than their whole shells; Figures 4a and 4b), and one on OJP that has experienced the most dissolution (ERDC 127, MFI = 0.83; *P. obliquiloculata* fragments are younger than their whole shells; Figures 4e and 4f). In these two samples the sediment is made up predominantly of fragments of foraminifers, and specimens of whole foraminifer shells are fewer. As dissolution proceeds, the radiocarbon age of whole, undamaged shells will lean toward the age of more sturdy

shells which likely have longer residence time in the mixed layer and are therefore older than coexisting fragments [*Le and Thunnell*, 1996; *Broecker and Clark*, 2001; modeling results from *Barker et al*., 2007]. So how is it that the fragments in these samples are younger than their whole shell counterparts?

[60] One mechanism may be interface dissolution [*Broecker et al*., 1991], or dissolution of new shells quickly upon arrival into the sediment which could cause the newly arriving shells to be fragmented. Simultaneously, bioturbation would bring older whole shells to the core top. Interface dissolution combined with bioturbation allows the fragments to be relatively young compared to whole shells in samples that have experienced greater dissolution.

[61] Another mechanism may be *sediment focusing*. Sediment redistribution is likely to cause robust whole shells to remain in situ [*Broecker et al*., 2006], and newly formed fragments and newly arriving lighter, porous foraminifers to be winnowed away because robust foraminifers are generally heavier than porous ones or fragments For example, in the 700–800 μm size range, average *G. sacculifer* weight is half that of *G. menardii* (Mekik unpublished data). This mechanism would give a younger age to the fragments compared to whole shells wherever the fragments are finally deposited.

[62] There are some caveats here, however. If the sand sized particles (like foraminifers and pteropod fragments) were going to be selectively sorted, one would expect to see evidence for transport in the form of laminations, ripples, removal of the finer-grained material, or increase in the sand fraction of the sediment. If evidence for fast bottom flow currents or other bathymetric features cannot be found, winnowing of lighter fragments would be an unrealistic hypothesis. A further caveat is that if fragments and lighter shells are winnowed a long distance and for a long time, they may become the older components in sediment wherever they finally become part of the sedimentary record. Experiments and more data on radiocarbon ages of fragments and whole shells in highly dissolved samples are needed to fully resolve the problem of why in highly dissolved sediments, fragments can be significantly younger than coexisting whole shells.

[63] In our down core data where ages of whole shells and fragments are compared (Figure 6), we see that fragments are consistently either the same age or older than whole shells; and the higher the average sediment accumulation rate of the core, the closer agreement is between the ages of fragments and whole shells. These results were predicted in previous work [e.g., *Barker et al*., 2007; *Broecker and Clark*, 2010, 2011] and reiterate that more reliable radiocarbon age estimates are produced in cores with higher accumulation rates and less dissolution.

[64] Pteropod fragments, where available in our samples, have the oldest ages of all other coexisting sedimentary components dated herein, both in core tops on RIO (Figure 3) and down core in MD98 2177 (Table 4). This may be surprising because pteropod shells are made of aragonite, a polymorph of calcite which is more soluble. In core tops on RIO in shallow water (such as, samples AII 107–9 66GGC and AII 107–9 69GGC) calcite dissolution is low because Δ calcite is high (37 to 43 μmol/kg). At this level of oversaturation, one would expect pteropod shells to be mostly intact, not fragmented as they are in core tops on RIO, and for this reason, to also be the youngest component of the sediment. So our counterintuitive results are puzzling.

[65] A possible explanation may be that these core tops are located at or below the aragonite saturation horizon, where interface dissolution causes the newly arriving aragonite shells to fragment and be winnowed away before becoming part of the sediments. As bioturbation continues to mix up older pteropod fragments, pteropod fragments may become the oldest component of the sediment. Based on the GLODAP database [*Key et al*., 2004], the Δ aragonite value (carbonate ion saturation with respect to aragonite) for the location of the two core tops on RIO are −2.69 and 6.29 μmol/kg, AII 107–9 66GGC and AII 107–9 69GGC, respectively. While one sample is below the aragonite saturation horizon (where Δ aragonite = 0), the other is not. More radiocarbon age data from pteropod fragments are necessary to resolve this issue.

[66] One last consideration may be that pteropods can live in a wide range of water depths (Table 2) and their radiocarbon ages may not be reflecting accurate reservoir corrections for their depth habitats. This issue is difficult to ascertain because it is impossible to identify which species a pteropod fragment belongs to in order to specify which water depth may have been its habitat waters.

4.5. Implications for the MFI Proxy

[67] The MFI proxy has been developed and applied in both core top [*Mekik et al*., 2007a, 2007b; *Mekik and Raterink*, 2008] and down core work [*Mekik et al*., 2012; *Doss and Marchitto*, 2013]. While fragments are expected to be older than whole shells as explained above, large age offsets between the fragments and whole shells of *G. menardii* would compromise the reliability of MFI in estimating percent calcite dissolved. Therefore, this issue became one of the main goals of the current study.

[68] Figure 4 illustrates that while fragments are consistently older than whole shells for *G. menardii*, the age offset is within 1000–1500 years in core tops (except in high dissolution samples and for the two samples of LGM age where the age offset between fragments and whole shells is ~3500 years). These age offsets are well within the range of age offsets among whole shells of coexisting species of foraminifers in the same core tops. On the RIO transect, the age offset between coexisting whole foraminifer tests is as high as 3500 years, and on the OJP transect it is close to 1000 years.

[69] In down core work (Figure 6), the age offset between fragments and whole shells of *G. menardii* is smaller in the two high-resolution cores (ME-27 and MD98-2177), but within the same offset range as core tops in the low sedimentation rate core (1000–1500 years in MW91-9-56). Thus, the age offset between the components of the MFI proxy is small enough to allow its use as a reliable indicator of percent calcite dissolved in both core top and down core work; and MFI is most reliable in cores with high sedimentation rate. Several issues remain, however.

[70] First, the radiocarbon age results for coexisting foraminifers and pteropods presented herein call for mechanisms such as chemical erosion and various types of dissolution (homogeneous, differential, and interface) occurring on the ocean floor and in the sediments. *Archer et al.'s* [2002] model used to calibrate MFI does not distinguish among these mechanisms. Instead, it calculates a percent calcite dissolved value for the bulk sediment. If the process or mechanism of dissolution varies from location to location, it becomes increasingly more difficult to use MFI or any other calcite

dissolution proxy which does not take these processes into account.

[71] Second, two core tops used herein are of LGM age (AII 107–9 149 and AII 107–9 133) possibly due to downslope mass transport of the previously overlying younger sediment. Another possibility is that the top of the cores may have been removed during the coring process. All core tops used herein are from gravity cores where such removal of the upper parts of the core may occur. We are confident that this is not a bioturbation-related artifact causing mixing of sediments from Marine Isotope Stage 5 because there is strong agreement between the ages of shells of three different species, *G. menardii*, *G. ruber*, and *G. truncatulinoides* in these samples. The two core tops of LGM age are part of the published calibration sample set for MFI which consists of 89 core tops from the Pacific, Atlantic, and Indian Oceans [*Mekik et al*., 2010]. Based on these new core top age results, two data points need to be removed from the calibration equation for MFI. Modifications to the MFI calibration equation will be investigated and published in a subsequent study.

[72] Third, radiocarbon dating is expensive and in many studies $\delta^{18}O$ data are used instead of $\Delta^{14}C$ to assess whether a core top is Holocene or Glacial in age. If the core top is Holocene, it is often considered to be "modern enough." This raises the question of what age is "too old" to be useful as a core top sample? Is it acceptable when calibrating proxies from deep sea sediments that core tops simply be Holocene even if they are as old as 7000 or 8000 years?

[73] Regardless of the calcite dissolution proxy used (whether MFI, SNSW, or other), core tops along a depth transect where dissolution increases downslope are required to calibrate the proxy. While dissolution will not alter the $^{14}C/^{12}C$ of the carbonate, as dissolution increases so does the age of the core top. Our results suggest that this may happen to such an extent that the proxies developed using aged core tops may no longer be analogous to parameters measured from the modern ocean. This is a problem inherent to quantifying calcite dissolution in deep sea sediments. The best way to quantify and calibrate calcite dissolution may be using microelectrodes to measure in situ calcite dissolution in sediment pore waters. This is an expensive method with limited or no down core applicability. Even if it were readily available, one would still be measuring calcite dissolution in older sediments.

[74] Moreover, this problem is not limited to calcite dissolution proxies. Calibrations for most proxies in paleoceanography are done with core tops ascertained to be of "modern" age; and data from these core tops are compared with a measurable parameter in the modern ocean (usually from databases like WOCE or GLODAP). Even if the calibration involves a calcite-based proxy that is not directly affected by dissolution, the calibration will be affected by the age of the core tops. Chemical erosion and interface dissolution may cause the calcareous components of the core tops to become older with increasing water depth. It would be erroneous to compare a carbonate-based proxy from older sediments with a modern oceanographic parameter.

[75] Core top calibration locations are often chosen strategically for the particular needs of the proxy being developed. While some proxies may be calibrated in samples that have experienced very little dissolution and/ or bioturbation, others may not. For example, a calibration location for a carbonate-based proxy measuring upwelling strength may be chosen in a region with high surface ocean productivity. However, high surface ocean productivity would lead to high organic carbon rain into the sediments, and organic carbon in the sediments would lead to metabolic respiratory dissolution of those sediments [*Emerson and Bender*, 1981; *Archer and Maier-Reimer*, 1994]. If the sediments are sufficiently dissolved by whatever mechanism, sediments will become older and the upwelling proxy would have to be calibrated with core tops that are not modern.

[76] All processes discussed herein which modify the age of coexisting components of sediments (e.g., chemical erosion, interface dissolution, bioturbation, etc.) create issues that affect many paleoceanographic proxies. This problem may be drawing limits to the accuracy of what can be achieved in paleoceanography where components of deep sea sediments are used to calibrate proxies.

[77] Lastly, it is somewhat surprising that the *G. menardii* shells on RIO are LGM in age because it was previously believed that *G. menardii* did not inhabit the Atlantic during Glacial times. *Sexton and Norris* [2011] recently reported *G. menardii* from the Glacial Atlantic, and we do also herein.

5. Conclusions

[78] Ideally there would be no age offset among any species of foraminifers, pteropods, or any other components of deep sea sediments within the same horizon in a given core. Multiple studies, including the present, have shown this to be untrue for many reasons. The most prevalent mechanism of sediment mixing is through bioturbation, although differential dissolution of shells, downslope mass transport, and sediment focusing are also important processes through which components of sediments are reworked and/or eroded.

[79] We find a consistent relationship of increasing radiocarbon age of foraminifer shells with increasing dissolution in our core tops. We also find that radiocarbon age offset is reduced in cores that have experienced little dissolution and have high sedimentation rates. In cores with lower accumulation rate, the age offset among coexisting components of the sediment is as high as 3500 years.

[80] Future work is necessary to better understand the mechanisms that create sediments where fragments of foraminifers are younger than coexisting whole shells, and where foraminifers bearing porous, fragile shells are older than those with sturdier tests. Perhaps the most pertinent remaining question for future studies are the following: shells of which planktonic foraminifer species produce the most reliable age estimates in sediments used in paleoceanographic work? Can an ideal method be established?

[81] **Acknowledgments.** This work benefited tremendously from discussions with Robert Anderson, Paul Loubere, and Daniel Sigman. We extend many thanks to Kathryn Elder and Susan Handwork at NOSAMS for their guidance. We are grateful to the core repositories providing samples to us; specifically June Padman and Bobbi Conard, Oregon State University; Larry Peterson, RSMAS; Rusty Lotti-Bond, Lamont Doherty Earth Observatory; Warren Smith, Scripps Institution of Oceanography; Ellen Roosen, Woods Hole Oceanographic Institution; and curators at the University of Hawaii. We thank the National Science Foundation for the support it provides to those repositories. We are also grateful to two anonymous reviewers for their thorough reviews and thoughtful comments which substantially improved this manuscript. This research was funded in full by National Science Foundation grants to Mekik, OCE0825280 and OCE1219739.

References

Adkins, J. F., and E. A. Boyle (1997), Changing atmospheric $\Delta^{14}C$ and the record of deep water paleoventilation ages, *Paleoceanography*, *12*, 237–344.

Anand, P., H. Elderfield, and M. H. Conte (2003), Calibration of Mg/Ca thermometry in planktonic foraminifera from a sediment trap time series, *Paleoceanography*, *18*(2), 1050, doi:10.1029/2002PA000846.

Archer, D., and E. Maier-Reimer (1994), Effect of deep sea sedimentary calcite preservation on atmospheric CO_2 concentration, *Nature*, *367*, 260–263.

Archer, D., J. L. Morford, and S. Emerson (2002), A model of suboxic sedimentary diagenesis suitable for automatic tuning and gridded global domains, *Global Biogeochem. Cycles*, *16*(1), 1017, doi:10.1029/2000GB001288.

Bard, E., M. Arnold, J. Duprat, J. Moyes, and J. C. Duplessy (1987), Reconstruction of the last deglaciation: Deconvoluted records of $\delta^{18}O$ profiles, micropaleontological variations and accelerator mass spectrometric ^{14}C dating, *Clim. Dyn.*, *1*, 101–112.

Barker, S., and H. Elderfield (2002), Foraminiferal calcification response to glacial-interglacial changes in atmospheric CO_2, *Science*, *297*, 833–836.

Barker, S., W. Broecker, E. Clark, and I. Hajdas (2007), Radiocarbon age offsets of foraminifera resulting from differential dissolution and fragmentation within the sedimentary bioturbated layer, *Paleoceanography*, *22*, PA2205, doi:10.1029/2006PA001354.

Be, A. W. H. (1960), Ecology of Recent planktonic foraminifera: Part 2—Bathymetric and seasonal distributions in the Sargasso Sea off Bermuda, *Micropaleontology*, *6*, 373–392.

Berger, W. H. (1970), Planktonic foraminifera: Selective solution and the lysocline, *Mar. Geol.*, *8*, 111–138.

Berger, W. H., and J. S. Killingley (1982), Box cores from the equatorial Pacific: 14C sedimentation rates and benthic mixing, *Mar. Geol.*, *45*, 93–125.

Berger, W. H., T. C. Johnson, and E. L. Hamilton (1977), Sedimentation on Ontong-Java Plateau: Observations on a classic "carbonate monitor", in *Fate of Fossil Fuel CO_2 in the Ocean*, edited by N. R. Anderson and A. Malahoff, pp. 543–567, Plenum Press, New York, NY.

Bijma, J. (1991), On the biology of tropicalspinose Globigerinidae (Sarcodina, Foraminiferida) and its implications for paleoecology, Thesis, 242 pp., Rijksuniv. Groningen, The Netherlands.

Broecker, W., and E. Clark (2001), An evaluation of Lohmann's foraminifera weight dissolution index, *Paleoceanography*, *16*, 531–534.

Broecker, W., and E. Clark (2010), Search for a Glacial age ^{14}C-depleted ocean reservoir, *Geophys. Res. Lett.*, *37*, L13606, doi:10.1029/2010GL043969.

Broecker, W., and E. Clark (2011), Radiocarbon age differences among coexisting planktic foraminifera shells: The Barker Effect, *Paleoceanography*, *26*, PA2222, doi:10.1029/2011PA002116.

Broecker, W. S., M. Klas, and E. Clark (1991), The influence of CaCO3 dissolution on the core top radiocarbon ages for deep sea sediments, *Paleoceanography*, *6*, 593–608.

Broecker, W. S., K. Matsumoto, E. Clark, I. Hajdas, and G. Bonani (1999), Radiocarbon age differences between coexisting foraminiferal species, *Paleoceanography*, *14*, 431–436.

Broecker, W., S. Barker, E. Clark, I. Hajdas, G. Bonani, and L. Stott (2004), Ventilation of the glacial deep Pacific Ocean, *Science*, *306*, 1169–1172.

Broecker, W., S. Barker, E. Clark, I. Hajdas, and G. Bonani (2006), Anomalous radiocarbon ages for foraminifera shells, *Paleoceanography*, *21*, PA2008, doi:10.1029/2005PA001212.

Doss, W., and T. Marchitto (2013), Glacial deep ocean sequestration of CO_2 driven by the eastern equatorial Pacific biologic pump, *Earth Planet. Sci. Lett.*, *377–378*, 43–54, doi:10.1016/j.epsl.2013.07.019.

Emerson, S., and M. Bender (1981), Carbon fluxes at the sediment water interface of the deep sea: Calcium carbonate preservation, *J. Mar. Res.*, *39*, 139–162.

Fairbanks, R. G., and P. Wiebe (1980), Foraminifera and chlorophyll maximum: Vertical distribution, seasonal succession, and paleoceanographic significance, *Nature*, *1524–1525*.

Fairbanks, R. G., M. Sverdlove, R. Free, P. H. Wiebe, and A. H. Be (1982), Vertical distribution and isotopic fractionation of living planktonic foraminifera from the Panama Basin, *Nature*, *298*, 841–844.

Farmer, E. C., A. Kaplan, P. B. deMenocal, and J. Lynch-Stieglitz (2007), Corroborating ecological depth preferences of planktic foraminifera in the tropical Atlantic with the stable oxygen isotope ratios of core top specimens, *Paleoceanography*, *22*, PA3205, doi:10.1029/2006PA001361.

Jasper, J. P., and W. G. Deuser (1993), Annual cycles of mass flux and isotopic composition of pteropod shells settling into the Sargasso Sea, *Deep Sea Res., Part I*, *40*, 653–669.

Jones, G. A., D. A. Johnson, and W. B. Curry (1984), High resolution stratigraphy in Late Pleistocene/Holocene sediments of the Vema Channel, *Mar. Geol.*, *58*, 59–87.

Juranek, L. W., A. D. Russell, and H. J. Spero (2003), Seasonal oxygen and carbon isotope variability in euthecosomatous pteropods from the Sargasso Sea, *Deep Sea Res., Part I*, *50*, 231–245.

Keigwin, L. D. (2004), Radiocarbon and stable isotope constraints on Last Glacial Maximum and Younger Dryas ventilation in the western North Atlantic, *Paleoceanography*, *19*, PA4012, doi:10.1029/2004PA001029.

Keir, R. (1984), Recent increase in Pacific $CaCO_3$ dissolution: A mechanism for generating old ^{14}C ages, *Mar. Geol.*, *59*, 227–250.

Keir, R., and R. L. Michel (1993), Interface dissolution control of the ^{14}C profile in marine sediment, *Geochim. Cosmochim. Acta*, *57*, 3563–3573.

Key, R. M., A. Kozyr, C. L. Sabine, K. Lee, R. Wanninkoff, J. L. Bullister, R. A. Feeley, F. J. Millero, C. Mordy, and T. H. Peng (2004), A global ocean carbon climatology results from Global Data Analysis Project (GLODAP), *Global Biogeochem. Cycles*, *18*, GB4031, doi:10.1029/2004GB002247.

Le, J. N., and R. C. Thunnell (1996), Modeling planktic foraminiferal assemblage changes and applications to sea surface temperature estimation in the western equatorial Pacific Ocean, *Mar. Micropaleontol.*, *28*, 211–229.

Loubere, P. (2001), Nutrient and oceanographic changes in the eastern equatorial Pacific from the last full glacial to the present, *Global Planet. Change*, *29*, 77–98.

Manighetti, B., I. N. McGave, M. Maslin, and N. J. Shackleton (1995), Chronology for climate change: Developing age models for the Biogeochemical Ocean Flux Study cores, *Paleoceanography*, *10*, 513–525.

Mekik, F., and R. François (2006), Tracing deep sea calcite dissolution: *Globorotalia menardii* fragmentation index and elemental ratios (Mg/Ca and Mg/Sr) in planktonic foraminifers, *Paleoceanography*, *21*, PA4219, doi:10.1029/2006PA001296.

Mekik, F., and L. Raterink (2008), Effects of surface ocean conditions on deep sea calcite dissolution dissolution proxies in the tropical Pacific, *Paleoceanography*, *23*, PA1216, doi:10.1029/2007PA001433.

Mekik, F., P. Loubere, and D. Archer (2002), Organic carbon flux and organic carbon to calcite flux ratio recorded in deep sea calcites: demonstration and a new proxy, *Global Biogeochem. Cycles*, *16*(3), 1052, doi:10.1029/2001GB001634.

Mekik, F., R. François, and M. Soon (2007a), A novel approach to dissolution correction of Mg/Ca-based paleothermometry in the tropical Pacific, *Paleoceanography*, *22*, PA3217, doi:10.1029/2007PA001504.

Mekik, F., P. Loubere, and M. Richaud (2007b), Rain ratio variation in the tropical ocean: Tests with surface sediments in the eastern equatorial Pacific, *Deep Sea Res., Part II*, *54*, 706–721, doi:10.1016/j.dsr2.2007.01.010.

Mekik, F., N. Noll, and M. Russo (2010), Progress toward a multi-basin calibration for quantifying deep sea calcite preservation in the tropical/subtropical world ocean, *Earth Planet. Sci. Lett.*, *299*, 104–117, doi:10.1016/j.epsl.2010.08.024.

Mekik, F., R. Anderson, P. Loubere, R. Francois, and M. Richaud (2012), The mystery of the missing deglacial carbonate preservation maximum, *Quat. Sci. Rev.*, *39*, 60–72, doi:10.1016/j.quascirev.2012.01.024.

Oxburgh, R. (1998), The Holocene preservation history of equatorial Pacific sediments, *Paleoceanography*, *13*, 50–62.

Peng, T. H., and W. S. Broecker (1984), The impacts of bioturbation on the age difference between benthic and planktonic foraminifera in deep sea sediments, *Nucl. Instrum. Methods Phys. Res., Sect. B*, *233*, 346–352.

Peng, T. H., W. S. Broecker, G. Kipphut, and N. J. Shackleton (1977), Benthic mixing in deep sea cores as determined by ^{14}C dating and its implications regarding climate stratigraphy and the fate of fossil fuel CO_2, in *The Fate of Fossil Fuel CO_2 in the Oceans*, edited by N. R. Anderson and A. Malahoff, pp. 355–373, Springer, New York.

Sabine, C. L., R. M. Key, A. Kozyr, R. A. Feeley, R. Wanninkof, F. J. Millero, T.-H. Peng, J. L. Bullister, and K. Lee (2005), Global Ocean Data Analysis Project: Results and data, ORNL/CDIAC-145, NDP-083, 110, Carbon Dioxide Information Analysis Center, Oak Ridge National Laboratory, U. S. Department of Energy, Oak Ridge, Tennessee, doi:10.3334/CDIAC/otg.ndp083.

Sadekov, A., S. M. Eggins, P. De Deckker, U. Ninnemann, W. Kuhnt, and F. Bassinot (2009), Surface and subsurface seawater temperature reconstruction using Mg/Ca microanalysis of planktonic foraminifera *Globigerinoides ruber*, *Globigerinoides sacculifer*, and *Pulleniatina obliquiloculata*, *Paleoceanography*, *24*, PA3201, doi:10.1029/2008PA001664.

Schlitzer, R. (2008), Ocean Data View. [Available at http://odv.awi.de].

Sexton, P. F., and R. D. Norris (2011), High latitude regulation of low latitude thermocline ventilation and planktic foraminifer populations across glacial-interglacial cycles, *Earth Planet. Sci. Lett.*, *311*, 69–81, doi:10.1016/j.epsl.2011.08.044.

Sikes, E. L., C. R. Samson, T. P. Guilderson, and W. R. Howard (2000), Old radiocarbon ages in the southwest Pacific ocean during the last glacial period ad deglaciation, *Nature*, *405*, 555–559.

Spero, H. J., and D. W. Lea (1993), Intraspecific stable isotope variability in the planktic foraminifera *Globigerinoides sacculifer*: Results from laboratory experiments, *Mar. Micropaleontol.*, *22*, 221–234.

Stuiver, M., and H. A. Polach (1977), Discussion Reporting of ^{14}C Data, *Radiocarbon*, *19*, 355–363.

Stuiver, M., and P. J. Reimer (1993), Extended ^{14}C data base and revised CALIB 3.0 ^{14}C age calibration program, *Radiocarbon*, *35*, 215–230.

Stuiver, M., P. J. Reimer, E. Bard, J. W. Bock, G. S. Burr, K. A. Hughen, B. Kromer, G. McCormac, J. Van der Picht, and M. Spark (1998), INTCAL98 radiocarbon age calibration, 24,000–0 cal BP, *Radiocarbon*, *40*, 1041–1083.

Waelbroeck, C., J. C. Duplessey, E. Michel, L. Labeyrie, D. Paillard, and J. Duprat (2001), The timing of the last deglaciation in North Atlantic climate records, *Nature*, *412*, 724–727.